Diverging roles for Lrp4 and Wnt signaling in neuromuscular synapse development during evolution

Leonor Remédio,[1] Katherine D. Gribble,[2] Jennifer K. Lee,[1] Natalie Kim,[1] Peter T. Hallock,[1] Nicolas Delestrée,[3,4,5] George Z. Mentis,[3,4,5] Robert C. Froemke,[1] Michael Granato,[2] and Steven J. Burden[1]

[1]Molecular Neurobiology Program, Helen L. and Martin S. Kimmel Center for Biology and Medicine at the Skirball Institute of Biomolecular Medicine, New York University Medical School, New York, New York 10016, USA; [2]Department of Cell and Developmental Biology, University of Pennsylvania Perelman School of Medicine, Philadelphia, Pennsylvania 19104, USA; [3]Center for Motor Neuron Biology and Disease, [4]Department of Pathology and Cell Biology, [5]Department of Neurology, Columbia University, New York, New York 10032, USA

Motor axons approach muscles that are prepatterned in the prospective synaptic region. In mice, prepatterning of acetylcholine receptors requires Lrp4, a LDLR family member, and MuSK, a receptor tyrosine kinase. Lrp4 can bind and stimulate MuSK, strongly suggesting that association between Lrp4 and MuSK, independent of additional ligands, initiates prepatterning in mice. In zebrafish, Wnts, which bind the Frizzled (Fz)-like domain in MuSK, are required for prepatterning, suggesting that Wnts may contribute to prepatterning and neuromuscular development in mammals. We show that prepatterning in mice requires Lrp4 but not the MuSK Fz-like domain. In contrast, prepatterning in zebrafish requires the MuSK Fz-like domain but not Lrp4. Despite these differences, neuromuscular synapse formation in zebrafish and mice share similar mechanisms, requiring Lrp4, MuSK, and neuronal Agrin but not the MuSK Fz-like domain or Wnt production from muscle. Our findings demonstrate that evolutionary divergent mechanisms establish muscle prepatterning in zebrafish and mice.

[*Keywords*: MuSK; Wnt; Frizzled; Lrp4; neuromuscular; synapse]

Supplemental material is available for this article.

Received February 17, 2016; revised version accepted March 31, 2016.

The formation and maintenance of the vertebrate neuromuscular synapse depend critically on Agrin, a ligand supplied by motor neurons. Agrin binds to Lrp4 in muscle, which promotes association between Lrp4 and MuSK, a receptor tyrosine kinase, stimulating MuSK phosphorylation (Burden et al. 2013). Once tyrosine-phosphorylated, MuSK initiates signaling cascades that promote synapse-specific transcription and anchoring of key postsynaptic proteins, including acetylcholine receptors (AChRs) (Lin et al. 2001; Burden et al. 2013). MuSK is a master regulator of synaptic differentiation, as MuSK activation not only stimulates postsynaptic differentiation but also controls presynaptic differentiation by anchoring and presenting Lrp4, which serves as a retrograde signal for differentiation of motor nerve terminals (Yumoto et al. 2012).

Synapse formation in vertebrates begins prior to the arrival of motor axons in muscle, as motor axons approach muscles that are specialized or prepatterned in the prospective synaptic region (for review, see Arber et al. 2002). Notably, *Lrp4*, *MuSK*, and *AChR* expression are enhanced in a narrow zone in the central region of mammalian muscle independently of innervation (Lin et al. 2001; Yang et al. 2001; Weatherbee et al. 2006; Kim and Burden 2008). Although AChR prepatterning is established independently of Agrin, prepatterning of mammalian muscle requires Lrp4 and MuSK (Yang et al. 2001; Weatherbee et al. 2006). In nonmammalian vertebrates, such as zebrafish, AChRs are likewise prepatterned in the central region of muscle in a MuSK-dependent manner (Flanagan-Steet et al. 2005; Panzer et al. 2006), preconfiguring the subsequent zone of innervation. Time-lapse imaging studies indicate that motor axons orient and grow toward this prepatterned zone (Panzer et al. 2006). Moreover, neuromuscular synapses form in a broader region of muscle in zebrafish that are deficient in prepatterning (Jing et al.

Corresponding authors: steve.burden@med.nyu.edu, leonor.remedio@med.nyu.edu
Article is online at http://www.genesdev.org/cgi/doi/10.1101/gad.279745.116.

2009). Consistent with these findings, forced, uniform expression of MuSK in mammalian muscle disrupts prepatterning and leads to exuberant motor axon growth and synapse formation throughout the muscle (Kim and Burden 2008). Together, these findings indicate that muscle prepatterning biases motor axon growth and synapse formation toward the central, prepatterned region of muscle.

Once motor axons make contact with muscle, motor axons provide opposing signals that refine and sharpen the prepatterned arrangement of AChRs. Agrin binds Lrp4, which stimulates further association between Lrp4 and MuSK and increases MuSK phosphorylation (Kim and Burden 2008; Zhang et al. 2008, 2011), essential to induce and maintain AChR clustering at nascent synaptic sites (for review, see Kummer et al. 2006; Burden et al. 2013). In contrast, ACh, acting in an antagonist manner, depolarizes muscle and extinguishes AChR clusters that are not directly apposed to nerve terminals that supply Agrin focally (Kummer et al. 2006; Burden et al. 2013).

The extracellular region of MuSK contains three Ig-like domains, a Frizzled (Fz)-like domain, and a short, unstructured juxtamembrane region (Burden et al. 2013). The first Ig-like domain is crucial for MuSK to associate with Lrp4 (Zhang et al. 2011). Autoantibodies to this first Ig-like domain disrupt binding between Lrp4 and MuSK and cause autoimmune MuSK myasthenia gravis (Huijbers et al. 2013; Koneczny et al. 2013). Because Fz receptors bind Wnts, the presence of a Fz-like domain in MuSK raised the possibility that Wnts may bind to the MuSK Fz-like domain and function as alternative ligands for MuSK (Koles and Budnik 2012). Several findings are consistent with the idea that Wnts promote one or more steps in synapse formation. First, Wnt proteins can bind MuSK (Jing et al. 2009; Strochlic et al. 2012; Zhang et al. 2012) in a manner that depends on the Fz-like domain (Jing et al. 2009; Strochlic et al. 2012). Second, Wnts can stimulate clustering of AChRs in cultured muscle cells in a MuSK-dependent manner (Henriquez et al. 2008; Zhang et al. 2012). Third, prepatterning of AChRs in zebrafish is dependent on the MuSK Fz-like domain as well as two Wnts, Wnt11r and Wnt4a, which are expressed by muscle (Jing et al. 2009; Gordon et al. 2012). Fourth, the development of neuromuscular synapses in *Drosophila* requires Wnt/Fz signaling and Neto (neuropilin and tolloid-like), an auxiliary subunit of glutamate receptors (Koles and Budnik 2012; Kim and Serpe 2013).

Although Wnts are required for AChR prepatterning in zebrafish (Jing et al. 2009), a role for Wnt signaling in prepatterning in mice has not been investigated. Because Lrp4 can bind and activate MuSK (Kim and Burden 2008), direct activation of MuSK by Lrp4 may be sufficient to stimulate MuSK phosphorylation and establish muscle prepatterning in mammals (Burden et al. 2013). An alternative model, supported by the findings in zebrafish, suggests that additional ligands, such as Wnts, assist or cooperate with Lrp4 and MuSK to activate MuSK and stimulate prepatterning in mammals. Moreover, although Wnt signaling is not required for synapse formation in zebrafish, a potential role for Wnt signaling in neuromuscular synapse formation in mammals has not been studied.

Here, we show that muscle prepatterning in zebrafish and mammals is established by different mechanisms. First, Lrp4 is required for prepatterning in mice but is dispensable in zebrafish. Second, Wnt signaling through the MuSK Fz-like domain is essential for prepatterning AChRs in zebrafish but is expendable in mice. The mechanisms for synapse formation, however, appear similar, as synapse formation in zebrafish and mice requires Lrp4 and MuSK, whereas the MuSK Fz-like domain and Wnt production from muscle are dispensable.

Results

Generation of a mouse MuSK mutant lacking the MuSK Fz-like domain

The MuSK Fz-like domain extends from Ser307 to Asp454 and is encoded by exons 9–12 (Fig. 1A,B). Exons 9–12 encode for two of the five amino acids between the third Ig-like domain and the Fz-like domain, the entire Fz-like domain, and seven of the 38 amino acids from the unstructured extracellular, juxtamembrane region (Fig. 1A,B). We used CRISPR/Cas9 to introduce double-strand breaks in introns 8 and 12, deleting 16.2 kb of DNA encoding the Fz-like domain and allowing splicing of RNA encoded by exons 8 and 13, which restores the reading frame (Fig. 1B).

To generate double-strand breaks in introns 8 and 12, we selected sgRNAs that were predicted to have a low probability to hybridize to off-target sites and tested and confirmed this expectation experimentally (see Supplemental Fig. S1A). We used PCR and DNA sequencing to analyze 25 mice born from zygotes injected with the sgRNAs and Cas9 mRNA (Fig. 1C). We found that 15 mice were heterozygous and that five mice were homozygous for the desired mutation in *MuSK* (Supplemental Fig. S1B). All mutations deleted exons 9–12 and led to nonhomologous end-joining of breaks in introns 8 and 12 and in-frame splicing of mRNA encoded by exons 8 and 13 (Supplemental Fig. S1C). Founder mice were mosaic for the *MuSK* mutation and harbored deletions of varying size at the double-strand break sites. As such, we backcrossed founder mice to wild-type mice to obtain lines that contained the expected sequence and only 2-, 11-, or 18-base-pair (bp) deletions at the double-strand break sites in introns 8 and 12 (Supplemental Fig. S1C).

Prepatterning of AChRs is very sensitive to MuSK expression levels and is nearly abolished in mice that are heterozygous for *MuSK* (Yang et al. 2001). Moreover, *MuSK* overexpression can lead to severe defects in motor axon growth, synapse formation, and motor performance (Kim and Burden 2008). As such, it was important to determine whether the MuSK ΔFz protein was expressed at normal levels. We generated primary muscle cell cultures from control and $MuSK^{\Delta Fz}$ mice, immunoprecipitated MuSK and MuSK ΔFz proteins with antibodies to the first Ig-like domain in MuSK, and detected MuSK and MuSK ΔFz proteins by probing Western blots with antibodies to the N terminus of MuSK. MuSK ΔFz protein expressed in either $MuSK^{\Delta Fz/+}$ or $MuSK^{\Delta Fz/\Delta Fz}$ myotubes migrated

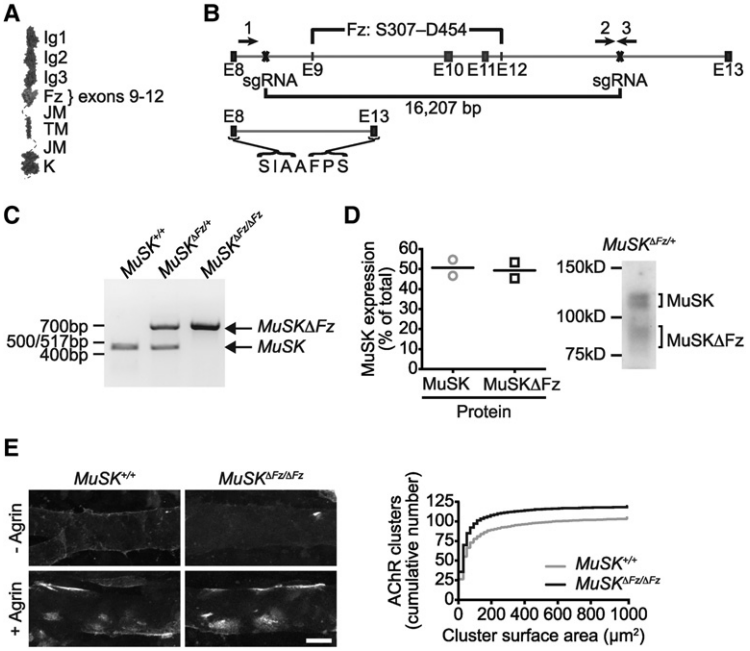

Figure 1. Generation of mice lacking the MuSK Fz-like domain. (*A*) The extracellular region of mammalian MuSK contains three Ig-like domains, a Fz-like domain encoded by exons 9–12, and a juxtamembrane (JM) region. Following the transmembrane (TM) domain, the intracellular region of MuSK contains a juxtamembrane region and a kinase (K) domain. (*B*) The schematic shows the strategy for deleting exons (E) 9–12, which encode the Fz-like domain (S307 to D454). The positions of the sgRNAs used to define the double-strand break sites (X) are indicated. The arrows show the positions of the primers (1–3) used for genotyping. Splicing of RNA encoded by exons 8 and 13 produces a protein that joins A304 to F463 and lacks the Fz-like domain. An A residue between A304 and F463 replaces two residues (EW) between the third Ig-like domain and the Fz-like domain as well as eight residues (YKKENITT) from the juxtamembrane region, which are encoded by exons 9 and 12. (*C*) Wild-type *MuSK* and $MuSK^{\Delta Fz}$ mutant alleles were detected by PCR. (*D*) Western blots from primary cultures of $MuSK^{\Delta Fz/+}$ myotubes show that MuSK ΔFz migrates at the predicted, truncated size and is expressed at the same level as wild-type MuSK ($n = 2$; each measurement is shown) (see also Supplemental Fig. S1). (*E*) Agrin stimulates AChR clustering in a similar manner in wild-type and $MuSK^{\Delta Fz/\Delta Fz}$ primary myotubes (wild-type, $n = 4$; $MuSK^{\Delta Fz/\Delta Fz}$, $n = 5$). Bar, 20 μm.

in SDS-PAGE at the predicted, truncated size (Fig. 1D; Supplemental Fig. S1D). We quantified expression of the MuSK ΔFz protein by comparing expression levels of the wild-type and MuSK ΔFz protein in $MuSK^{\Delta Fz/+}$ myotubes. This assay provided a reliable and accurate comparison of protein expression, as we measured wild-type and MuSK ΔFz protein expression within individual myotube cultures and avoided the inevitable variability caused by immunoprecipitating and comparing MuSK expression in separate cultures of wild-type and $MuSK^{\Delta Fz/\Delta Fz}$ myotubes. Importantly, we found that MuSK ΔFz and wild-type MuSK proteins are expressed at the same level (Fig. 1D), ensuring that potential defects in prepatterning or synapse formation in $MuSK^{\Delta Fz/\Delta Fz}$ mice would be caused by a loss of the Fz-like domain rather than an alteration in MuSK expression.

We measured the responsiveness of MuSK ΔFz to neural Agrin by measuring the number and size of AChR clusters that formed in primary myotubes following Agrin treatment. We found that the number and size of Agrin-induced AChR clusters were similar in myotubes expressing MuSK ΔFz or wild-type MuSK (Fig. 1E). These findings indicate that deletion of the Fz-like domain did not impair the ability of MuSK to associate with Lrp4 and initiate downstream signaling pathways that organize and anchor AChRs in response to Agrin.

The MuSK Fz-like domain is not essential for muscle prepatterning

In mammals, motor axons arrive and make contact with muscle shortly after muscle prepatterning is established. Motor axons then provide multiple signals that refine and sharpen the muscle prepattern (Flanagan-Steet et al. 2005; Kummer et al. 2006). For these reasons, it is difficult to define and unravel requirements for prepatterning AChRs separately from mechanisms for clustering AChRs during synapse formation by studying wild-type mice with intact innervation. Therefore, to study the role of the MuSK Fz-like domain in muscle prepatterning, we generated mice that were homozygous mutant for MuSK ΔFz and also lacked motor neurons. As in the past, we generated "motor neuron-less" mice by expressing diphtheria toxin A (DTA) selectively in motor neurons, which ablates motor neurons before they extend motor axons into the periphery (Yang et al. 2001). We dissected muscle from embryonic day 17.5–18.5 (E17.5–E18.5) mice, 1–2 d before birth, and stained diaphragm muscles with probes that labeled axons and AChRs. Figure 2 shows that AChRs are clustered and enriched in the central region of muscle in wild-type and $MuSK^{\Delta Fz/\Delta Fz}$ mice that lack motor axons, demonstrating that the MuSK ΔFz-like domain is not essential for muscle prepatterning. The distribution of prepatterned AChR clusters, however, is modestly broader in mice lacking the MuSK Fz-like domain: In wild-type mice, 50% of AChR clusters are contained in a 567-μm-wide zone in the center of the muscle, whereas the width of this zone is modestly expanded to 750 μm in $MuSK^{\Delta Fz/\Delta Fz}$ mice (Fig. 2B). These findings indicate that the MuSK Fz-like domain is not required for muscle prepatterning but contributes to shaping the prepatterned zone within the central region of the muscle (see the Discussion).

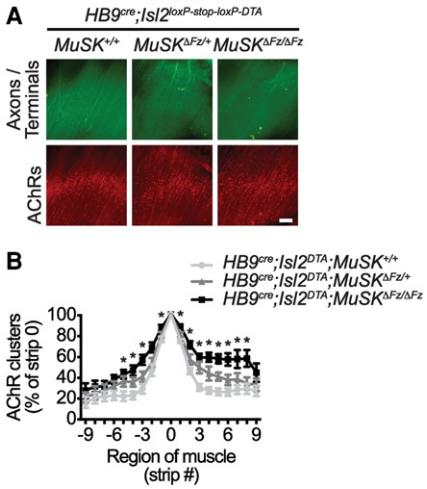

Figure 2. The MuSK Fz-like domain is not essential for muscle prepatterning. (*A*) AChR expression is enriched in the central region of the diaphragm muscle from mice that lack motor neurons (*HB9*^{cre}; *Isl2*$^{loxP\text{-}stop\text{-}loxP\text{-}DTA}$; *MuSK*$^{+/+}$). AChR expression is also prepatterned in mice that lack motor neurons and are heterozygous (*HB9*^{cre}; *Isl2*$^{loxP\text{-}stop\text{-}loxP\text{-}DTA}$; *MuSK*$^{\Delta Fz/+}$) or homozygous (*HB9*^{cre}; *Isl2*$^{loxP\text{-}stop\text{-}loxP\text{-}DTA}$; *MuSK*$^{\Delta Fz/\Delta Fz}$) mutant for MuSK$^{\Delta Fz}$. (*B*) The distribution of the prepatterned AChRs is modestly wider in *MuSK*$^{\Delta Fz/\Delta Fz}$ mice than in wild-type mice ($n = 6$; mean ± SEM, [*] $P < 0.05$) but is normal in *MuSK*$^{\Delta Fz/+}$ mice ($P = 0.3$). Diaphragm muscles from E17.5 or E18.5 mice were stained with antibodies to Neurofilament and Synapsin to label axons and with α-bungarotoxin (α-BGT) to label AChRs. The remaining axons at the periphery of the muscle are likely sensory and/or autonomic axons. Bar, 250 µm.

Synapse formation is normal in mice lacking the MuSK Fz-like domain

Neuromuscular function becomes essential for survival at birth, when mice first need to breathe on their own. To determine whether neuromuscular synapses failed to form or function, we intercrossed *MuSK*$^{\Delta Fz/+}$ mice and measured lethality. We found that homozygous *MuSK*$^{\Delta Fz/\Delta Fz}$ mice were born at the expected Mendelian frequency (Supplemental Fig. S1E), suggesting that neuromuscular function was not severely perturbed. To study the structure of neuromuscular synapses, we intercrossed *MuSK*$^{\Delta Fz/+}$ mice and stained muscle from postnatal day 0 (P0), P21, and P60 mice with probes that label axons, nerve terminals, and AChRs. Plaque-shaped synapses, indistinguishable from those in wild-type mice, were present in *MuSK*$^{\Delta Fz/\Delta Fz}$ mice at birth and matured to form complex, pretzel-shaped synapses over the next month. The structure of the synapse in *MuSK*$^{\Delta Fz/\Delta Fz}$ mice continued to evolve over the following month in a manner indistinguishable from wild-type mice and was maintained in adults. We measured the width of the endplate zone at birth and the synaptic size and the density of synaptic AChRs at each age. We found that *MuSK*$^{\Delta Fz/\Delta Fz}$ mice were normal in each aspect (Fig. 3). Thus, the formation and maturation of neuromuscular synapses do not depend on signaling through the MuSK Fz-like domain.

Synaptic function is normal in mice lacking the MuSK Fz-like domain

To determine whether synaptic transmission was normal in mice lacking the MuSK Fz-like domain, we recorded from individual muscle fibers with intracellular microelectrodes to measure the amplitude and frequency of spontaneous miniature end-plate potentials (mepps). In addition, we used extracellular electrodes to measure nerve-elicited compound muscle action potentials (CMAPs) in muscle. We found that the muscle resting potential and the amplitude and frequency of mepps were indistinguishable between wild-type and *MuSK*$^{\Delta Fz/\Delta Fz}$ mice (Fig. 4A). Likewise, CMAPs, following stimulation at 10–50 Hz, were normal in *MuSK*$^{\Delta Fz/\Delta Fz}$ mice (Fig. 4B; Supplemental Fig. S2). Thus, the MuSK Fz-like domain is not required for the cardinal features of synaptic transmission.

To determine whether motor function was perturbed in mice lacking the MuSK Fz-like domain, we measured motor performance using multiple motor function tests. We found that the performance of *MuSK*$^{\Delta Fz/\Delta Fz}$ mice on RotaRod, wire hang, all limb, and forelimb grip strength assays were normal, consistent with the idea that synaptic transmission and muscle function do not require signaling through the MuSK Fz-like domain (Fig. 4C).

Wnt secretion from muscle is dispensable for synapse formation in mice

Binding of Wnts to MuSK depends on the MuSK Fz-like domain (Jing et al. 2009; Strochlic et al. 2012). Because the MuSK Fz-like domain is expendable for synaptic differentiation (Fig. 3), our findings demonstrate that Wnt signaling through MuSK is not required for synapse formation. We wondered, however, whether Wnts were also dispensable or might act through bona fide Fz receptors to regulate synapse formation in mice. Because 19 *Wnt* genes are expressed in mammals, we studied mice that that were deficient in Wnt secretion by generating mice that were conditionally mutant for *Wntless* (*Wls*), which is required for secretion of lipid-modified Wnt proteins (Port and Basler 2010). We studied mice that were deficient in Wnt secretion from muscle tissue by generating *Pax3*^{cre}; *Wls*$^{loxP/loxP}$ mice to inhibit Wnt secretion from skeletal muscle cells and *Scx::cre; Wls*$^{loxP/loxP}$ mice to inhibit Wnt secretion from tendon precursors and muscle interstitial cells. *Pax3*^{cre}; *Wls*$^{loxP/loxP}$ mice were runted and displayed several overt structural abnormalities, including malformations of the head, the absence of a tail, and incomplete closure of the neural tube (Fig. 5A), consistent with described roles for Wnt-3a, Wnt-5a, and Dvl1/2 during mouse development (Takada et al. 1994; Gofflot et al. 1998; Yamaguchi et al. 1999; Hamblet et al. 2002). However, the pattern of AChR expression, axon branching, and nerve terminals was normal (Fig. 5B). Moreover, each AChR cluster was apposed by a nerve terminal, indicating that ACh-mediated disassembly of noncontacted AChR clusters occurred normally (Fig. 5C). Similarly, synapse formation was normal in *Scx::cre; Wls*$^{loxP/loxP}$ mice

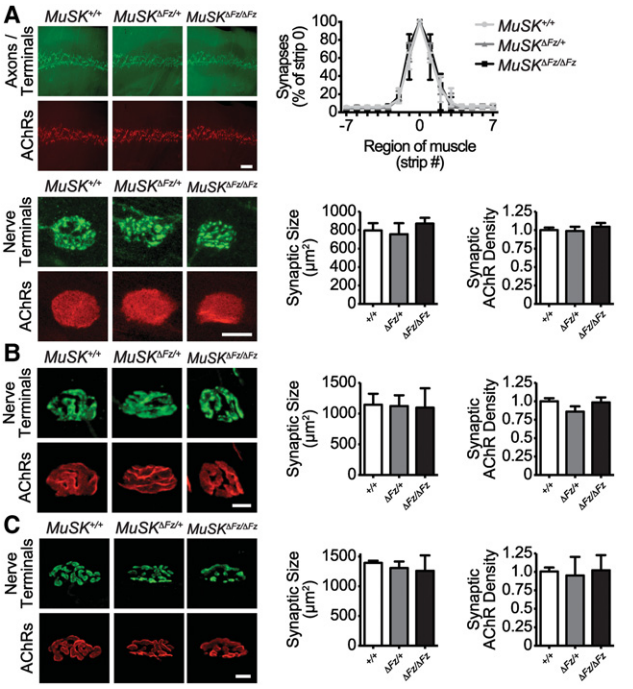

Figure 3. The MuSK Fz-like domain is dispensable for synapse formation and maturation. (*A*) The positions of motor axons, nerve terminals, AChRs, and synapses are similar in diaphragm muscles from P0 wild-type, $MuSK^{\Delta Fz/+}$, and $MuSK^{\Delta Fz/\Delta Fz}$ mice ($n = 4$; median and interquartile range, $P > 0.05$). (*A–C*) The shape and arrangement of neuromuscular synapses is normal in $MuSK^{\Delta Fz/+}$ and $MuSK^{\Delta Fz/\Delta Fz}$ mice at P0 (*A*), P21 (*B*), and P60 (*C*). Synaptic size and the density of synaptic AChRs are normal at each age. We analyzed 50–280 synapses from three to six mice at each age for each genotype (median and interquartile range, $P > 0.08$). Bars: *A*, *top* panels, 250 µm; *B*,*C*, *bottom* panels, 10 µm.

(Fig. 5C). Although we cannot exclude the possibility that a low level of Wnt secretion from muscle occurs in the absence of Wls, these findings indicate that Wnt secretion from the major cell types in skeletal muscle tissue—namely, skeletal muscle cells, muscle interstitial cells, and tendon cells—is not required for neuromuscular synapse formation in mice.

Wnt4 and Wnt11 are not required for synapse formation in mice

Zebrafish require Wnt4a and Wnt11r as well as the MuSK Fz-like domain for muscle prepatterning (Jing et al. 2009; Gordon et al. 2012). Our studies of muscle conditional *Wls* mutant mice left open the possibility that Wnt4 or Wnt11, the closest mammalian homolog of zebrafish Wnt11r, might be produced by nonmuscle cell types and control muscle prepatterning or synapse formation. We therefore studied mice that lack Wnt4 and Wnt11. In *Wnt11* mutant mice, motor axons branch excessively within the diaphragm muscle but establish synapses with muscle in a zone marked by AChR clusters that is only modestly wider than normal (Fig. 5D,E). Synapse formation appears normal in *Wnt4* mutant mice, and the width of the synaptic zone was as wide in *Wnt11*/*Wnt4* double mutant mice as in *Wnt11* mutant mice (Fig. 5E). These findings indicate that neither Wnt11 nor Wnt4 plays key roles in synapse formation in mice.

Ectopic muscle islands form within the central tendon of the diaphragm muscle in *Wnt11* mutant mice (Fig. 5F). These ectopic muscle islands are usually innervated, forming a typical synaptic zone in the middle of the ectopic muscle islands, indicating that Wnt11 is also dispensable for synapse formation of these ectopic muscles. Occasionally, ectopic islands are not innervated (Fig. 5F), which provided an opportunity to study the potential role of Wnt11 in nerve-independent muscle prepatterning. We found that AChR clusters are highly enriched in the middle of the noninnervated ectopic muscle islands (Fig. 5F), indicating that Wnt11 is not essential for muscle prepatterning.

Zebrafish Lrp4 is required for synapse formation but not prepatterning

Previous studies reported that Lrp4 is necessary for prepatterning in mice (Weatherbee et al. 2006). In zebrafish, Wnt signaling through the MuSK Fz-like domain is required for prepatterning AChRs. We therefore wondered whether muscle prepatterning in zebrafish is controlled exclusively by a Wnt-dependent mechanism or whether Lrp4 also has a role in prepatterning in zebrafish. We used TALENS to generate two zebrafish *lrp4* mutant alleles with premature stop codons following the LDLa repeats, thus deleting most of the MuSK- and Agrin-binding domains (Fig. 6A,B). Importantly, these zebrafish *lrp4* alleles closely resemble the mouse *Lrp4* mutant allele lacking prepatterning and synapse formation (Weatherbee et al. 2006).

In zebrafish embryos, prepatterned AChR clusters form in the central region of adaxial muscle cells prior to the arrival of motor axons, ~16 h post-fertilization (hpf) (Flanagan-Steet et al. 2005; Panzer et al. 2006). As motor neuron growth cones traverse the muscle territory, between 17 and 29 hpf, some of the aneural AChR clusters become incorporated into stable en passant neuromuscular synapses (Flanagan-Steet et al. 2005).

We stained *lrp4* mutant zebrafish embryos at 19.5 hpf with α-bungarotoxin (α-BGT) and an antibody (znp-1) to Synaptotagmin2 and found that AChR clusters were present in *lrp4* mutant and wild-type sibling embryos (Fig. 6C,C′). We measured the width of the band of prepatterned AChR clusters relative to the width of each hemisegment and found no difference between wild-type and *lrp4* mutant embryos (wild-type, $n = 17$ hemisegments, 20.17% ± 1.24%; *lrp4* mutant, $n = 30$ hemisegments, 21.73% ± 1.16%; mean ± SEM, $P = 0.4$, unpaired Student's *t*-test). These findings indicate that zebrafish use a Wnt–MuSK signaling mechanism, exclusive of Lrp4, for muscle prepatterning. However, Lrp4 is required for neuromuscular synapse formation in zebrafish, as en passant synapses between motor axons and axial muscles fail to form in the absence of Lrp4 (Fig. 6D,D′), demonstrating that Lrp4 has a conserved and essential role in synapse formation in lower

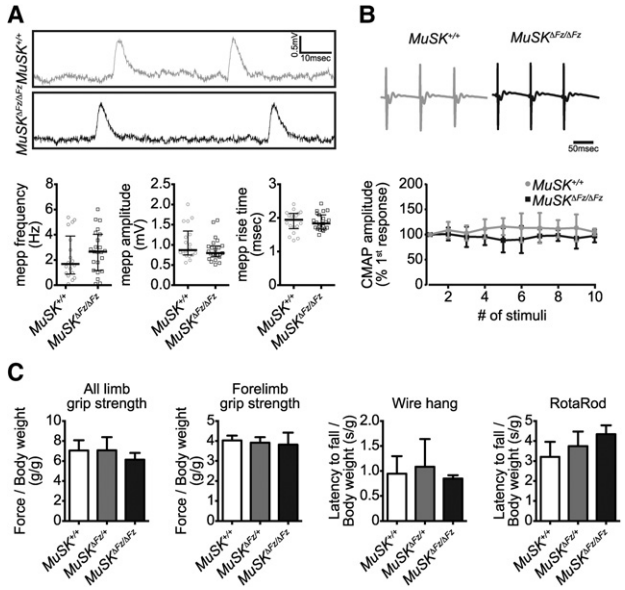

Figure 4. The MuSK Fz-like domain is dispensable for normal synaptic transmission. (*A*) The amplitude and frequency of mepps were indistinguishable between wild-type and $MuSK^{\Delta Fz/\Delta Fz}$ P30 mice. $n = 4$ mice of each genotype; median and interquartile range, $P > 0.05$. (*B*) The CMAP in the tibialis anterior muscle, following stimulation of the peroneal nerve at 10 Hz, was normal in $MuSK^{\Delta Fz/\Delta Fz}$ P14 mice (see also Supplemental Fig. S2). The last three CMAPs of the stimulation trains are shown. Changes in CMAP amplitude are plotted as a percentage of the amplitude of the first response. $n = 5$ mice of each genotype; mean ± SEM, $P > 0.05$. (*C*) Motor performance of P60 male $MuSK^{\Delta Fz/+}$ and $MuSK^{\Delta Fz/\Delta Fz}$ mice were normal, as assessed by two grip strength, wire hang, and RotaRod assays. $n = 4$; median and interquartile range, $P > 0.05$.

and higher vertebrates. A few abnormally shaped AChR clusters remain on the surface of muscle pioneer cells in *lrp4* mutants (Fig. 6D′, white arrowheads), although the significance of these clusters is unknown.

In mammals, *Lrp4* is expressed as myoblasts begin to fuse to form multinucleated fibers and prior to innervation (Kim et al. 2008). We therefore wondered whether *lrp4* is expressed in early muscle development and during the prepatterning stage in zebrafish embryos. Using RNAscope, which is optimized to detect low-level transcripts, we found that *lrp4* mRNA is not detectable at the prepatterning stage (Fig. 6E) but is readily detectable when neuromuscular synapses are forming (Fig. 6E′). These findings are consistent with our data showing that Lrp4 is not required for AChR prepatterning in zebrafish and indicate that the timing of *lrp4* expression in muscle differs in zebrafish and mice.

Lrp4 is required for AChR prepatterning in mice

The differing roles for Lrp4 in prepatterning in zebrafish and mice led us to revisit the reported role for Lrp4 in muscle prepatterning in mice. Although AChR clustering is absent in *Lrp4* mutant mice at E14.5 (Weatherbee et al. 2006), motor axons are already present within the muscle at this stage. Because neuronal ACh disassembles AChR clusters that are not sustained by Agrin/MuSK signaling (Flanagan-Steet et al. 2005; Kummer et al. 2006), we wondered whether an acceleration of ACh-mediated disassembly rather than a failure to initially prepattern AChRs might be responsible for an absence of AChR clusters in *Lrp4* mutant mice at this stage. To study the role of Lrp4 in nerve-independent prepatterning, we generated mice that lack Lrp4 as well as

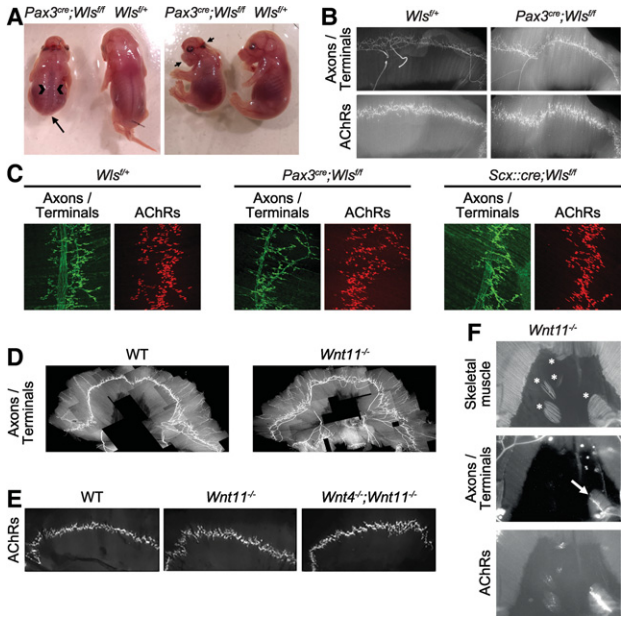

Figure 5. Wnt11, Wnt4a, and Wnt secretion from muscle is dispensable for neuromuscular synapse formation. (*A*) $Pax3^{cre}$; $Wls^{f/f}$ E18.5 mice deficient in Wnt secretion from skeletal muscle cells were runted and displayed several overt structural abnormalities, including malformations of the head (short arrows), the absence of a tail (long arrow), and incomplete closure of the neural tube (brackets), consistent with reported roles for Wnt-3a and Wnt-5a in mouse development. (*B*) The pattern of AChR expression and motor axon branching are normal in mice deficient in Wnt secretion from skeletal muscle. (*C*) Nerve terminals form in apposition to AChR clusters in $Pax3^{cre}$; $Wls^{f/f}$ E18.5 mice deficient in Wnt secretion from skeletal muscle cells and in *Scx::cre;* $Wls^{f/f}$ E18.5 mice deficient in Wnt secretion from tendon precursors and muscle interstitial cells. (*D*) Branching from the main intramuscular nerve is effusive in *Wnt11* mutant mice. (*E*) The band of synaptic AChR expression is modestly broader in *Wnt11* mutant mice than wild-type mice but expanded no further in mice that are mutant for both Wnt4 and Wnt11. (*F*) AChR expression is enriched at synapses and prepatterned in noninnervated ectopic muscles that form within the central tendon of *Wnt11* mutant mice. The positions of ectopic muscle islands (stained for myosin [MHC]) are indicated (*). One of the ectopic islands is innervated (arrow), as revealed by staining for axons and nerve terminals (Synaptophysin/Synapsin), whereas the other islands are not innervated. AChRs are clustered in both the central, synaptic zone in innervated muscle and the middle of the noninnervated ectopic muscle islands.

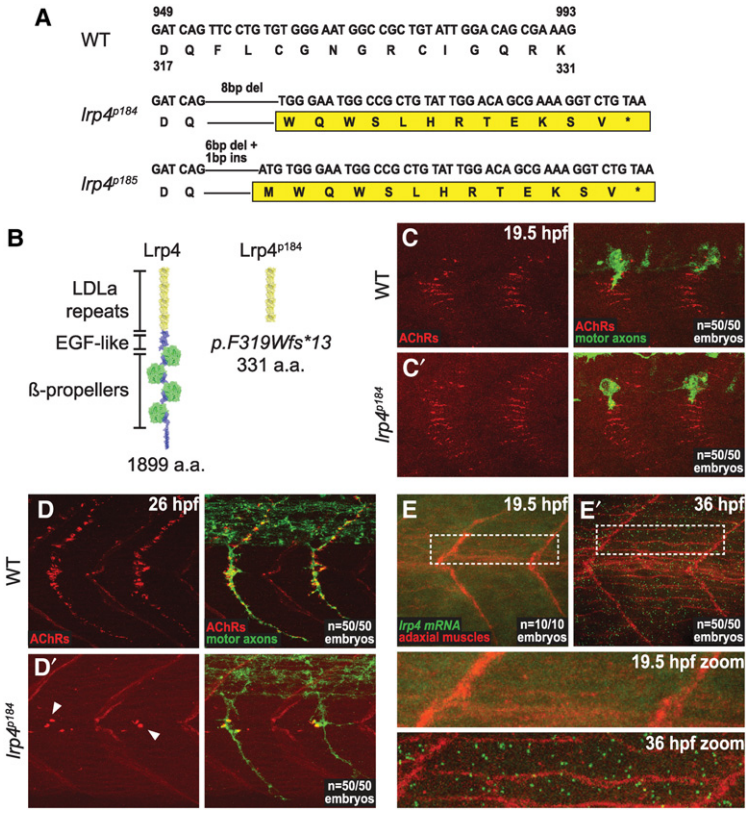

Figure 6. Zebrafish Lrp4 is required for synapse formation but not AChR prepatterning. (*A*) Sequences of wild-type zebrafish *lrp4* exon 9 and sequences of $lrp4^{p184}$ and $lrp4^{p185}$, two frameshift alleles that were generated using TALENs targeting exon 9. (*B*) The protein domain structure of wild-type zebrafish Lrp4 (1899 amino acids) and the predicted structure of $lrp4^{p184}$ (331 amino acids), which resembles the mouse *mitt* allele and is predicted to lack the β-propeller domains, the EGF-like domains, the transmembrane domain, and the intracellular region. (*C*,*C*′) Lateral views of wild-type and *lrp4* mutant zebrafish embryos at the prepatterning stage (19.5 h post-fertilization [hpf]) stained for AChRs (red) and motor axons (green). *Lrp4* mutant embryos show no reduction or defect in AChR prepatterning. $n = 50$ out of 50 embryos. (*D*,*D*′) Lateral views of wild-type and *lrp4* mutant zebrafish embryos at the synapse formation stage (26 hpf) stained for AChRs (red) and motor axons (green). In contrast to the prepatterning stage, *lrp4* mutant embryos show a significant reduction in AChRs clustered beneath the motor axon terminals, with only a few "hot spot" AChR clusters remaining at the horizontal myoseptum (white arrowheads). $n = 50$ out of 50 embryos. (*E*,*E*′) Lateral views of in situ hybridizations performed on wild-type zebrafish embryos at the prepatterning stage (*E*) and synapse formation stage (*E*′). *Lrp4* mRNA expression is undetectable at the prepatterning stage (*E* and zoomed panel) but robustly expressed at later stages (*E*′ and zoomed panel), consistent with a requirement for zebrafish Lrp4 during synapse formation but not during prepatterning.

motor neurons. Figure 7 shows that AChRs fail to cluster in muscle from mice that lack Lrp4 and motor innervation. These findings confirm and extend the earlier findings and demonstrate that Lrp4 has a critical role in prepatterning AChRs in mice but not in zebrafish (Weatherbee et al. 2006).

Discussion

The extracellular region of mammalian MuSK possesses three Ig-like domains and a Fz-like domain. One face of the first Ig-like domain is hydrophobic and has a critical role in MuSK dimerization, whereas the opposing, solvent-exposed surface is critical for association of MuSK with Lrp4 (Stiegler et al. 2006). As such, the first Ig-like domain plays an essential role in stimulation of MuSK by Agrin, which is crucial for synapse formation. The presence of a Fz-like domain in MuSK led to speculation that Wnts may bind to MuSK and regulate MuSK activity at one or more stages during synapse formation (Masiakowski and Yancopoulos 1998; Xu and Nusse 1998; Koles and Budnik 2012; Barik et al. 2014). Consistent with this idea, the MuSK Fz-like domain as well as Wnt4 and Wnt11r play important roles in muscle prepatterning in zebrafish (Jing et al. 2009). Here, however, we show that the MuSK Fz-like domain is dispensable for muscle prepatterning and synapse formation in mice. Moreover, we show that Lrp4 is required for prepatterning in mice but not in zebrafish. These findings indicate that prepatterning is established by different mechanisms in mice and zebrafish. In mice, Lrp4, which binds to MuSK and stimulates MuSK phosphorylation (Kim et al. 2008), is essential for muscle prepatterning. In contrast, prepatterning in zebrafish depends on Wnt signaling through the MuSK Fz-like domain and does not require Lrp4. Thus, different *cis*-acting ligands activate MuSK during prepatterning in zebrafish and mice: Muscle-derived Wnts function as MuSK ligands in zebrafish, while Lrp4 serves as the *cis*-acting ligand for MuSK in mice. The requirements for synapse formation,

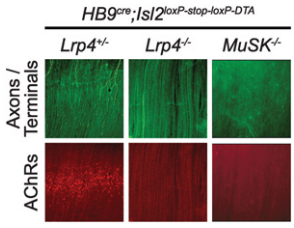

Figure 7. AChR prepatterning is absent in *Lrp4* mutant mice. AChRs are prepatterned in the middle of muscle from E18.5 mice that lack motor neurons but are wild type or heterozygous for *Lrp4*. AChR prepatterning is absent in E18.5 mice that lack motor neurons and are homozygous mutant for *MuSK* or *Lrp4*. Motor neurons were eliminated by expressing DTA from HB9-expressing motor neurons ($HB9^{cre}$; $Isl2^{loxP\text{-}stop\text{-}loxP\text{-}DTA}$), and axons and terminals were stained with antibodies to Neurofilament and Synapsin. The stained axons at the edges of the muscle are likely sensory and/or autonomic.

however, are similar in zebrafish and mice, as Lrp4 and MuSK, but not the MuSK Fz-like domain, play essential roles in synapse formation.

We found that synapse formation and motor performance are normal in mice lacking the MuSK Fz-like domain, similar to findings in zebrafish (Jing et al. 2009). A recent study reported that prepatterned AChRs were almost undetectable and that synapse formation and motor performance were severely impaired in mice that are mutant for the MuSK Fz-like domain (Messéant et al. 2015). However, Messéant et al. (2015) did not examine the patterning of AChR expression prior to or independent of innervation. Even at the earliest stage examined by Messéant et al. (2015), motor axons had innervated the diaphragm muscle, precluding investigation of the role of the MuSK Fz-like domain in muscle prepatterning. It is unclear what accounts for the strikingly differing findings on synapse formation and motor performance reported here and in the study from Messéant et al. (2015). We note that the MuSK ΔFz mutant described in Messéant et al. (2015) lacked amino acids 305–453 and was substantially overexpressed, as the 85-kDa mutant protein was shown to be much more abundant than the ~110-kDa wild-type protein. In contrast, the MuSK Δ305–461 protein described here is expressed at normal levels. We speculate that overexpression of the MuSK Δ305–453 protein in Messéant et al. (2015) may be due to an abnormal stability of the mutant protein or mRNA; alternatively, splicing of RNA encoded by exons 8 and 12 may be unusually efficient, resulting in higher levels of mRNA expression. Increases in MuSK expression cause severe defects in AChR clustering, motor axon growth, synapse formation, and motor performance (Kim and Burden 2008), similar to the defects reported by Messéant et al. (2015). Thus, MuSK overexpression rather than the loss of the Fz-like domain may be responsible for the defects in synapse formation and motor function described in the previous study. Future studies—in particular to determine whether MuSK Δ305–453 heterozygotes display a phenotype indicating a gain-of-function mutation rather than a loss-of-function mutation—will be important for resolving these issues.

We found that AChR clusters are prepatterned in a modestly broader zone in mice lacking the MuSK Fz-like domain. These results indicate that signaling through the MuSK Fz-like domain is not necessary but participates to restrict AChR expression to the central region of mammalian muscle. These findings raise the possibility that a remnant of the older, Wnt-dependent mechanism, critical for prepatterning AChRs in fish, may be retained in mammals but has become subservient to Lrp4.

Injection of cells that express Sfrp, which binds and sequesters Wnts and inhibits Wnt-dependent signaling, in chick embryos leads to a twofold reduction in the number of AChR clusters in muscle (Henriquez et al. 2008). Because Sfrp-expressing cells were injected at Hamburger-Hamilton stage 24/25, before synapses form in chick embryos, and analyzed at Hamburger-Hamilton 27/28, when synapses first begin to form (Landmesser and Morris 1975), Wnts may have a role in regulating AChR expression and prepatterning during muscle development in chicks as well as zebrafish.

Lrp4 functions bidirectionally at mammalian neuromuscular synapses. Lrp4 binds neuronal Agrin to stimulate postsynaptic differentiation and signals in turn in a retrograde manner to motor axons to stimulate presynaptic differentiation (Weatherbee et al. 2006; Kim et al. 2008; Zhang et al. 2008; Yumoto et al. 2012). In the absence of Lrp4, like in the absence of MuSK, mammalian motor axons fail to stop and differentiate and instead wander aimlessly across muscle (DeChiara et al. 1996; Weatherbee et al. 2006). In zebrafish, Lrp4 may not have the same critical role for stimulating presynaptic differentiation, as motor axons display only a modest axon branching in the absence of Lrp4. Thus, Lrp4 appears to have acquired two new functions during vertebrate evolution: an effective activator of MuSK to stimulate muscle prepatterning and an essential retrograde signal to stimulate presynaptic differentiation. Because MuSK is required for accurate pathfinding and neuromuscular synapse formation in zebrafish, activation of MuSK by Wnts may lead to the production or presentation of a novel retrograde signal for differentiation of pioneering motor axons in zebrafish.

Motor axons within the main intramuscular nerve defasciculate and branch excessively in *Wnt11* mutant mice but not in *Wls* conditionally mutant mice that are deficient in Wnt secretion from muscle. These findings indicate that the axon defasciculation and branching defects in *Wnt11* mutant mice are not due to a loss of Wnt11 produced by muscle cells. Because Schwann cells express *Wnt11* (Sienknecht and Fekete 2008) and because similar axon defasciculation and branching defects are evident in mutant mice that are deficient in the migration of Schwann cell precursors to the periphery (Morris et al. 1999; Woldeyesus et al. 1999; Yang et al. 2001), Wnt11 may be required for Schwann cell survival, migration, or signaling to motor axons.

What mechanisms underlie the change in the role for Lrp4 in muscle prepatterning during vertebrate evolution? The simplest explanation appears to be a shift in the timing of *lrp4* expression, since *lrp4* expression is not evident in zebrafish muscle when prepatterning is established, whereas *lrp4* is expressed early in muscle development in mice. In addition, the association between Lrp4 and MuSK independently of Agrin may have increased during evolution, allowing Lrp4 to function as an effective ligand for MuSK. In this regard, although the extracellular region of Lrp4 is well conserved (80% identity) between mice and zebrafish, the extracellular region of MuSK is less well conserved (43% identity). Mammalian MuSK contains three Ig-like domains and a Fz-like domain (Burden et al. 2013), whereas MuSK in all other vertebrate classes, including fish, contains an additional, kringle domain (Jennings et al. 1993; Valenzuela et al. 1995; Fu et al. 1999; Ip et al. 2000). The addition of a kringle domain in zebrafish MuSK accounts for substantial sequence dissimilarity between the extracellular regions of zebrafish and mouse MuSK, as the sequences of the Ig-like and Fz-like domains are 55% identical. The function of the kringle domain is

not known, but it may impede binding between Lrp4 and MuSK, rendering prepatterning in nonmammalian vertebrates less sensitive to Lrp4 and necessitating a distinct, Wnt-dependent mechanism for stimulating MuSK prior to innervation. Because Lrp4 is required for synapse formation in zebrafish and mammals, potential interference by the kringle domain would presumably be overcome by Agrin binding to Lrp4.

The Fz-like domain is an ancient motif (Yan et al. 2014) that is present, together with a kringle domain, in a pair of mammalian receptor tyrosine kinases, Ror1/2, which have homologs in *Drosophila* and *Caenorhabditis elegans*. Although the function of the *Drosophila* homologs *Dror* (Wilson et al. 1993) and *Dnrk* (Oishi et al. 1997) are not known, CAM-1 and, in particular, the Fz-like domain in CAM-1 have an important role in neural development in *C. elegans* (Forrester et al. 1999; Kim and Forrester 2003; Green et al. 2007; Hayashi et al. 2009). Thus, it is interesting to speculate that MuSK evolved from these ancestral invertebrate kinases but diverged so that the Ig-like domain and kinase activity rather than the Fz-like and kringle domains became central to MuSK function.

Materials and methods

Animals and histology

Mice were housed and maintained according to Institutional Animal Care and Use Committee (IACUC) guidelines. *HB9^{cre}*, *Pax3^{cre}*, *Scx::cre*, *Isl2$^{loxP\text{-}stop\text{-}loxP\text{-}DTA}$*, *Lrp4* mutant, *MuSK* mutant, *Wnt4* mutant, *Wnt11* mutant, and *Wls* conditionally mutant mice have been described previously (Stark et al. 1994; DeChiara et al. 1996; Yang et al. 2001; Majumdar et al. 2003; Lang et al. 2005; Weatherbee et al. 2006; Blitz et al. 2009). In order to delete exons 9–12 in *MuSK*, we selected sgRNAs that were predicted to hybridize selectively to sequences in introns 8 and 12 of *MuSK* (http://crispr.mit.edu). We tested three pairs of sgRNAs by transfecting mouse embryonic stem cells with DNA encoding the sgRNAs together with Cas9 and found that each sgRNA pair was effective in directing deletion of the desired sequence in *MuSK*. We chose one sgRNA pair to delete exons 9–12 in zygotes (intron 8, GGTCTGCAAGCGTCCTAGTG; and intron 12, GGCAGTTAGGCAGGCGTCAT). The sgRNA pair (50 ng/µL) and 100 ng/µL Cas9 RNA were transcribed in vitro and injected into C57BL/6N zygotes. We analyzed 25 mice that were born from injected zygotes by PCR (primer 1, GCATGCCCA CAAAGGTGAAA; primer 2, TAGGGGGCATGGAGGATG TT; and primer 3, TGGGCAGAGTGAGAGTGTGA) and DNA sequencing of tail DNA. Fifteen of the 25 mice carried one *MuSK* allele with a deletion of exons 9–12, and five of the 25 mice carried two mutant *MuSK* alleles. We crossed three of the founder mice to wild-type mice to generate three F1 lines. Each line lacks exons 9–12 in *MuSK*, due to nonhomologous end-joining of breaks in introns 8 and 12; the three lines contained small deletions (2, 11, or 18 bp) at the break sites in introns 8 and 12. DNA sequencing from these lines confirmed the sequence of the *MuSK* mutations, which led to joining of introns 8 and 12, deletion of exons 9–12, and in-frame splicing of RNA encoded by exons 8 and 13 (Fig. 1). We analyzed seven genomic loci that scored the highest probability for off-target recognition by the chosen sgRNAs (http://crispr.mit.edu) by amplifying tail DNA of F1 mice and sequencing a 1-kb region, which was centered on the predicted off-site sequence (Supplemental Fig. S1A). We found no evidence for mutations in these genes (Supplemental Fig. S1A).

Zebrafish strains and animal care

Zebrafish *lrp4^{p184}* and *lrp4^{p185}* alleles were generated in the TLF background, and all wild-type fish used were TLF strain. Homozygous mutants obtained by crossing heterozygous carriers were identified at 36 hpf based on swimming motility defects in response to light touch. Both *lrp4^{p184}* and *lrp4^{p185}* alleles showed identical prepatterning and neuromuscular phenotypes; only the results from the *lrp4^{p184}* allele are shown. All fish were raised and maintained as described previously (Mullins et al. 1994). We performed all experiments involving fish according to animal protocols that were approved by the University of Pennsylvania IACUC.

Generation of TALEN mutant alleles

TALE nuclease plasmids were designed and engineered by the University of Utah Mutation Generation and Detection Core Facility and subcloned into pCS2TAL3-DDD and pCS2TAL3-RRR. The left TALEN was designed to target the sequence 5′-TCCTCCATGTGCGCCCGAT-3′. The right TALEN was designed to target the sequence 5′-ATGGCCGCTGTATTGG ACA-3′. Lrp4 TALEN mRNA was transcribed using the SP6 mMessage mMachine Kit (Ambion) and was diluted to 50 pg in 0.1 M KCl and microinjected into one-cell stage TLF embryos. Successful dsDNA breaks in *lrp4* of G0 injected embryos were confirmed by PCR and high-resolution melt analysis. Heterozygous F1 carrier alleles were identified and characterized by PCR followed by high-resolution melt analysis and sequencing (Dahlem et al. 2012).

Histology

Whole mounts of diaphragm muscles from P0, P21, and P60 mice were stained with Alexa 594-conjugated α-BGT (Invitrogen) to label AChRs and with antibodies to Neurofilament-L (SYnaptic SYstems) and Synaptophysin (Zymed) or Synapsin 1/2 (SYnaptic SYstems) to label motor axons and nerve terminals, respectively (Kim and Burden 2008). Images were acquired with a Zeiss LSM 700 or 800 confocal microscope, and the number and size of AChR clusters as well as the density of synaptic AChRs were determined using Volocity 3D imaging software (Perkin Elmer), as described previously (Jaworski and Burden 2006; Friese et al. 2007). The Wilcoxon-Mann-Whitney test was used to determine statistical significance and was conducted using GraphPad Prism 6.0 software.

Low-magnification images were captured on a Zeiss Axio Zoom.V16 fluorescence stereomicroscope. The distributions of prepatterned AChRs and synapses were determined by measuring the pixel value in 100-µm strips of the diaphragm muscle using Fiji software, as described previously (Kim and Burden 2008). We used the Kruskal-Wallis test with Bonferroni correction to determine whether differences in median values were statistically significant ($P < 0.05$).

Zebrafish embryos at 19–26 hpf were anesthetized in 0.01% Tricaine, fixed in 4% paraformaldehyde with 1% DMSO diluted in phosphate-buffered saline (1× PBS at pH 7.4) for 3 h at room temperature, and washed with PBS. Embryos were permeabilized using 0.1% collagenase for 3–7 min at room temperature and then washed thoroughly with PBS. To label AChR clusters, embryos were incubated for 3 h at 4°C in 10 µg/mL Alexa fluor 594-conjugated α-BGT (Molecular Probes) diluted in incubation buffer (0.2% BSA, 0.5% Triton X-100 in 1× PBS) with 1% normal goat

serum added. Motor axons were labeled with the znp-1 antibody (1:200) overnight at 4°C followed by incubation with goat anti-mouse secondary Alexa fluor 488-conjugated antibody (1:500). Stained embryos were immersed overnight and subsequently mounted in VectaShield mounting medium (Vector Laboratories). Embryos were imaged in 1-µm sections using a 60× immersion objective on a Zeiss LSM 710 confocal microscope. Image stacks were compressed into maximum intensity projections in Fiji and converted to 16-bit images using MetaMorph (Molecular Devices). AChR clusters were counted using the "count nuclei" function with minimum/maximum length set at 4/30 and minimum average intensity set at 15. The results were recorded in Graphpad Prism for statistical analysis.

In situ hybridization was performed using the RNAscope kit (Advanced Cell Diagnostics) in whole zebrafish embryos expressing *Tg(smyhc1:mCherry-CAAX)* as described (Gross-Thebing et al. 2014). Probes against *lrp4* were designed and engineered by Advanced Cell Diagnostics. Embryos were imaged in 1-µm sections on a 60× immersion objective on an Olympus spinning disk confocal microscope. Image stacks were compressed into maximum intensity projections and processed using Adobe Photoshop to adjust brightness and contrast.

Cell culture

Skin and bone were removed from limbs of E17.5–E18.5 embryos, and the remaining tissue was dissociated and plated on collagen/laminin-coated tissue culture dishes (750 µg of collagen, 3.3 µg of laminin per milliliter), as described previously (Smith et al. 2001). After several days, the growth medium (80% DMEM/F12, 20% fetal bovine serum [Gibco], 1:500 primocin [InvivoGen], 5 pg/mL bFGF [Invitrogen]) was exchanged for differentiation medium (95% DMEM/F12, 5% heat-inactivated horse serum [Gibco], 1:500 primocin).

Several days after myotubes had formed, the cultures were treated for 8 h with 0.5 nM recombinant neural Agrin-B8 (R&D Systems) and stained with Alexa 594 α-BGT to label AChRs and with antibodies to myosin heavy chain (MyHC) (Sigma) to measure myotube surface area. Images were collected using a Zeiss LSM 800 confocal microscope, and the number and size of AChR clusters, normalized to MyHC-stained myotube surface area, were determined using Volocity 3D imaging software, as described previously (Friese et al. 2007).

Alternatively, myotube lysates were prepared as described previously (Friese et al. 2007), and MuSK was immunoprecipitated from cleared lysates with antibodies to the first Ig-like domain in MuSK (Huijbers et al. 2013). The antibody/MuSK complex was captured with protein A-agarose beads (Roche). Following several washes, bound proteins were eluted from the beads with SDS sample buffer, heated for 5 min to 95°C, resolved by SDS-PAGE, and transferred to PVDF membranes (Herbst and Burden 2000). Membranes were blocked in Tris-buffered saline with 0.05% Tween-20 and 2% BSA and probed with rabbit antibodies to the N terminus (GTEKLPKAPVITTPLETVDA) of mammalian MuSK diluted in blocking buffer. Antibody binding to MuSK was detected with secondary horseradish peroxidase conjugated-mouse anti-rabbit IgG (Jackson ImmunoResearch) and quantified using a ChemiDoc imaging system (Bio-Rad).

Electrophysiology

We recorded from diaphragm muscles of postnatal 4-wk-old mice using standard intracellular microelectrodes and measured the frequency and amplitude of spontaneous mepps, as described previously (Jevsek et al. 2006; Friese et al. 2007). We recorded from 18 to 23 muscle fibers from four mice of each genotype.

In addition, we stimulated the common peroneal nerve from P14 mice at low (10-Hz), medium (25-Hz), and high (50-Hz) frequencies and used an extracellular electrode to record the CMAP from the tibialis anterior muscle. We used the Wilcoxon-Mann-Whitney test to determine whether differences in the mean values were significant ($P < 0.05$).

Behavior

Forelimb and all limb muscle strength was determined in P60 male mice using a grip force tensiometer (Bioseb). Mice held by their tails were allowed to grip a grid that was connected to the grip strength meter, and the mice were gently pulled horizontally until their grip was released. Five trials were conducted; forelimb and all limb tests were separated by a 20- to 30-min interval. We averaged the force (*g*) from the three maximum scores and normalized this value to body weight (g).

Motor function of P60 male mice was assessed on a RotaRod (AccuRotor four-channel, Omnitech Electronics, Inc.). Mice were placed on the RotaRod (3.0-cm rotating cylinder) rotating at 2.5 rpm, and the speed of rotation was increased linearly to 40 rpm over the course of 5 min. The time to fall from the rod was measured. Each mouse was subjected to three trials in 5-min intervals, and we recorded the longest latency to fall from the three trials.

We assessed motor fatigue in P60 male mice using an inverted wire hang test. Individual mice were placed on a wire, which was supported by two columns 27 cm apart, mounted 60 cm above a padded laboratory bench. After gently placing the forelimbs on the wire, the time to fall from the wire was measured. We recorded the longest latency to fall from three trials, separated by 15–30 min. We used the Kruskal-Wallis test to determine whether differences in the median values were significant ($P < 0.05$).

Acknowledgments

We are grateful to Dr. Sang Yong Kim, director of the Rodent Genetic Engineering Core at New York University Medical School, for his assistance in generating the $MuSK^{\Delta Fz}$ mice described here. We thank Kyle Tessier-Lavigne for initial steps in designing the CRISPR/Cas9 mutagenesis strategy, Elena Michaels for aiding with the mouse colony management, Dr. Michael Cammer for advice with image analysis, and Dr. Adam Mar (director of the Rodent Behavior Core at New York University Medical School) and Begona Gamallo-Lana for their assistance with the motor performance tests.

References

Arber S, Burden SJ, Harris AJ. 2002. Patterning of skeletal muscle. *Curr Opin Neurobiol* **12:** 100–103.

Barik A, Zhang B, Sohal GS, Xiong WC, Mei L. 2014. Crosstalk between Agrin and Wnt signaling pathways in development of vertebrate neuromuscular junction. *Dev Neurobiol* **74:** 828–838.

Blitz E, Viukov S, Sharir A, Shwartz Y, Galloway JL, Pryce BA, Johnson RL, Tabin CJ, Schweitzer R, Zelzer E. 2009. Bone ridge patterning during musculoskeletal assembly is mediated through SCX regulation of Bmp4 at the tendon-skeleton junction. *Dev Cell* **17:** 861–873.

Burden SJ, Yumoto N, Zhang W. 2013. The role of MuSK in synapse formation and neuromuscular disease. *Cold Spring Harb Perspect Biol* **5:** a009167.

Dahlem TJ, Hoshijima K, Jurynec MJ, Gunther D, Starker CG, Locke AS, Weis AM, Voytas DF, Grunwald DJ. 2012. Simple methods for generating and detecting locus-specific mutations induced with TALENs in the zebrafish genome. *PLoS Genet* **8:** e1002861.

DeChiara TM, Bowen DC, Valenzuela DM, Simmons MV, Poueymirou WT, Thomas S, Kinetz E, Compton DL, Rojas E, Park JS, et al. 1996. The receptor tyrosine kinase MuSK is required for neuromuscular junction formation in vivo. *Cell* **85:** 501–512.

Flanagan-Steet H, Fox MA, Meyer D, Sanes JR. 2005. Neuromuscular synapses can form in vivo by incorporation of initially aneural postsynaptic specializations. *Development* **132:** 4471–4481.

Forrester WC, Dell M, Perens E, Garriga G. 1999. A *C. elegans* Ror receptor tyrosine kinase regulates cell motility and asymmetric cell division. *Nature* **400:** 881–885.

Friese MB, Blagden CS, Burden SJ. 2007. Synaptic differentiation is defective in mice lacking acetylcholine receptor β-subunit tyrosine phosphorylation. *Development* **134:** 4167–4176.

Fu AK, Smith FD, Zhou H, Chu AH, Tsim KW, Peng BH, Ip NY. 1999. *Xenopus* muscle-specific kinase: molecular cloning and prominent expression in neural tissues during early embryonic development. *Eur J Neurosci* **11:** 373–382.

Gofflot F, Hall M, Morriss-Kay GM. 1998. Genetic patterning of the posterior neuropore region of curly tail mouse embryos: deficiency of Wnt5a expression. *Int J Dev Biol* **42:** 637–644.

Gordon LR, Gribble KD, Syrett CM, Granato M. 2012. Initiation of synapse formation by Wnt-induced MuSK endocytosis. *Development* **139:** 1023–1033.

Green JL, Inoue T, Sternberg PW. 2007. The *C. elegans* ROR receptor tyrosine kinase, CAM-1, non-autonomously inhibits the Wnt pathway. *Development* **134:** 4053–4062.

Gross-Thebing T, Paksa A, Raz E. 2014. Simultaneous high-resolution detection of multiple transcripts combined with localization of proteins in whole-mount embryos. *BMC Biol* **12:** 55.

Hamblet NS, Lijam N, Ruiz-Lozano P, Wang J, Yang Y, Luo Z, Mei L, Chien KR, Sussman DJ, Wynshaw-Boris A. 2002. Dishevelled 2 is essential for cardiac outflow tract development, somite segmentation and neural tube closure. *Development* **129:** 5827–5838.

Hayashi Y, Hirotsu T, Iwata R, Kage-Nakadai E, Kunitomo H, Ishihara T, Iino Y, Kubo T. 2009. A trophic role for Wnt–Ror kinase signaling during developmental pruning in *Caenorhabditis elegans*. *Nat Neurosci* **12:** 981–987.

Henriquez JP, Webb A, Bence M, Bildsoe H, Sahores M, Hughes SM, Salinas PC. 2008. Wnt signaling promotes AChR aggregation at the neuromuscular synapse in collaboration with agrin. *Proc Natl Acad Sci* **105:** 18812–18817.

Herbst R, Burden SJ. 2000. The juxtamembrane region of MuSK has a critical role in agrin-mediated signaling. *EMBO J* **19:** 67–77.

Huijbers MG, Zhang W, Klooster R, Niks EH, Friese MB, Straasheijm KR, Thijssen PE, Vrolijk H, Plomp JJ, Vogels P, et al. 2013. MuSK IgG4 autoantibodies cause myasthenia gravis by inhibiting binding between MuSK and Lrp4. *Proc Natl Acad Sci* **110:** 20783–20788.

Ip FC, Glass DG, Gies DR, Cheung J, Lai KO, Fu AK, Yancopoulos GD, Ip NY. 2000. Cloning and characterization of muscle-specific kinase in chicken. *Mol Cell Neurosci* **16:** 661–673.

Jaworski A, Burden SJ. 2006. Neuromuscular synapse formation in mice lacking motor neuron- and skeletal muscle-derived Neuregulin-1. *J Neurosci* **26:** 655–661.

Jennings CG, Dyer SM, Burden SJ. 1993. Muscle-specific trk-related receptor with a kringle domain defines a distinct class of receptor tyrosine kinases. *Proc Natl Acad Sci* **90:** 2895–2899.

Jevsek M, Jaworski A, Polo-Parada L, Kim N, Fan J, Landmesser LT, Burden SJ. 2006. CD24 is expressed by myofiber synaptic nuclei and regulates synaptic transmission. *Proc Natl Acad Sci* **103:** 6374–6379.

Jing L, Lefebvre JL, Gordon LR, Granato M. 2009. Wnt signals organize synaptic prepattern and axon guidance through the zebrafish unplugged/MuSK receptor. *Neuron* **61:** 721–733.

Kim N, Burden SJ. 2008. MuSK controls where motor axons grow and form synapses. *Nat Neurosci* **11:** 19–27.

Kim C, Forrester WC. 2003. Functional analysis of the domains of the *C elegans* Ror receptor tyrosine kinase CAM-1. *Dev Biol* **264:** 376–390.

Kim YJ, Serpe M. 2013. Building a synapse: a complex matter. *Fly (Austin)* **7:** 146–152.

Kim N, Stiegler AL, Cameron TO, Hallock PT, Gomez AM, Huang JH, Hubbard SR, Dustin ML, Burden SJ. 2008. Lrp4 is a receptor for Agrin and forms a complex with MuSK. *Cell* **135:** 334–342.

Koles K, Budnik V. 2012. Wnt signaling in neuromuscular junction development. *Cold Spring Harb Perspect Biol* **4:** a008045.

Koneczny I, Cossins J, Waters P, Beeson D, Vincent A. 2013. MuSK myasthenia gravis IgG4 disrupts the interaction of LRP4 with MuSK but both IgG4 and IgG1-3 can disperse preformed agrin-independent AChR clusters. *PLoS One* **8:** e80695.

Kummer TT, Misgeld T, Sanes JR. 2006. Assembly of the postsynaptic membrane at the neuromuscular junction: paradigm lost. *Curr Opin Neurobiol* **16:** 74–82.

Landmesser L, Morris DG. 1975. The development of functional innervation in the hind limb of the chick embryo. *J Physiol* **249:** 301–326.

Lang D, Lu MM, Huang L, Engleka KA, Zhang M, Chu EY, Lipner S, Skoultchi A, Millar SE, Epstein JA. 2005. Pax3 functions at a nodal point in melanocyte stem cell differentiation. *Nature* **433:** 884–887.

Lin W, Burgess RW, Dominguez B, Pfaff SL, Sanes JR, Lee KF. 2001. Distinct roles of nerve and muscle in postsynaptic differentiation of the neuromuscular synapse. *Nature* **410:** 1057–1064.

Majumdar A, Vainio S, Kispert A, McMahon J, McMahon AP. 2003. Wnt11 and Ret/Gdnf pathways cooperate in regulating ureteric branching during metanephric kidney development. *Development* **130:** 3175–3185.

Masiakowski P, Yancopoulos GD. 1998. The Wnt receptor CRD domain is also found in MuSK and related orphan receptor tyrosine kinases. *Curr Biol* **8:** R407.

Messéant J, Dobbertin A, Girard E, Delers P, Manuel M, Mangione F, Schmitt A, Le Denmat D, Molgo J, Zytnicki D, et al. 2015. MuSK frizzled-like domain is critical for mammalian neuromuscular junction formation and maintenance. *J Neurosci* **35:** 4926–4941.

Morris JK, Lin W, Hauser C, Marchuk Y, Getman D, Lee KF. 1999. Rescue of the cardiac defect in ErbB2 mutant mice reveals essential roles of ErbB2 in peripheral nervous system development. *Neuron* **23:** 273–283.

Mullins MC, Hammerschmidt M, Haffter P, Nusslein-Volhard C. 1994. Large-scale mutagenesis in the zebrafish: in search of

genes controlling development in a vertebrate. *Curr Biol* **4:** 189–202.

Oishi I, Sugiyama S, Liu ZJ, Yamamura H, Nishida Y, Minami Y. 1997. A novel *Drosophila* receptor tyrosine kinase expressed specifically in the nervous system. Unique structural features and implication in developmental signaling. *J Biol Chem* **272:** 11916–11923.

Panzer JA, Song Y, Balice-Gordon RJ. 2006. In vivo imaging of preferential motor axon outgrowth to and synaptogenesis at prepatterned acetylcholine receptor clusters in embryonic zebrafish skeletal muscle. *J Neurosci* **26:** 934–947.

Port F, Basler K. 2010. Wnt trafficking: new insights into Wnt maturation, secretion and spreading. *Traffic* **11:** 1265–1271.

Sienknecht UJ, Fekete DM. 2008. Comprehensive Wnt-related gene expression during cochlear duct development in chicken. *J Comp Neurol* **510:** 378–395.

Smith CL, Mittaud P, Prescott ED, Fuhrer C, Burden SJ. 2001. Src, Fyn, and Yes are not required for neuromuscular synapse formation but are necessary for stabilization of agrin-induced clusters of acetylcholine receptors. *J Neurosci* **21:** 3151–3160.

Stark K, Vainio S, Vassileva G, McMahon AP. 1994. Epithelial transformation of metanephric mesenchyme in the developing kidney regulated by Wnt-4. *Nature* **372:** 679–683.

Stiegler AL, Burden SJ, Hubbard SR. 2006. Crystal structure of the agrin-responsive immunoglobulin-like domains 1 and 2 of the receptor tyrosine kinase MuSK. *J Mol Biol* **364:** 424–433.

Strochlic L, Falk J, Goillot E, Sigoillot S, Bourgeois F, Delers P, Rouviere J, Swain A, Castellani V, Schaeffer L, et al. 2012. Wnt4 participates in the formation of vertebrate neuromuscular junction. *PLoS One* **7:** e29976.

Takada S, Stark KL, Shea MJ, Vassileva G, McMahon JA, McMahon AP. 1994. Wnt-3a regulates somite and tailbud formation in the mouse embryo. *Genes Dev* **8:** 174–189.

Valenzuela DM, Stitt TN, DiStefano PS, Rojas E, Mattsson K, Compton DL, Nunez L, Park JS, Stark JL, Gies DR, et al. 1995. Receptor tyrosine kinase specific for the skeletal muscle lineage: expression in embryonic muscle, at the neuromuscular junction, and after injury. *Neuron* **15:** 573–584.

Weatherbee SD, Anderson KV, Niswander LA. 2006. LDL-receptor-related protein 4 is crucial for formation of the neuromuscular junction. *Development* **133:** 4993–5000.

Wilson C, Goberdhan DC, Steller H. 1993. Dror, a potential neurotrophic receptor gene, encodes a *Drosophila* homolog of the vertebrate Ror family of Trk-related receptor tyrosine kinases. *Proc Natl Acad Sci* **90:** 7109–7113.

Woldeyesus MT, Britsch S, Riethmacher D, Xu L, Sonnenberg-Riethmacher E, Abou-Rebyeh F, Harvey R, Caroni P, Birchmeier C. 1999. Peripheral nervous system defects in erbB2 mutants following genetic rescue of heart development. *Genes Dev* **13:** 2538–2548.

Xu YK, Nusse R. 1998. The Frizzled CRD domain is conserved in diverse proteins including several receptor tyrosine kinases. *Curr Biol* **8:** R405–R406.

Yamaguchi TP, Bradley A, McMahon AP, Jones S. 1999. A Wnt5a pathway underlies outgrowth of multiple structures in the vertebrate embryo. *Development* **126:** 1211–1223.

Yan J, Jia H, Ma Z, Ye H, Zhou M, Su L, Liu J, Guo AY. 2014. The evolutionary analysis reveals domain fusion of proteins with Frizzled-like CRD domain. *Gene* **533:** 229–239.

Yang X, Arber S, William C, Li L, Tanabe Y, Jessell TM, Birchmeier C, Burden SJ. 2001. Patterning of muscle acetylcholine receptor gene expression in the absence of motor innervation. *Neuron* **30:** 399–410.

Yumoto N, Kim N, Burden SJ. 2012. Lrp4 is a retrograde signal for presynaptic differentiation at neuromuscular synapses. *Nature* **489:** 438–442.

Zhang B, Luo S, Wang Q, Suzuki T, Xiong WC, Mei L. 2008. LRP4 serves as a coreceptor of agrin. *Neuron* **60:** 285–297.

Zhang W, Coldefy AS, Hubbard SR, Burden SJ. 2011. Agrin binds to the N-terminal region of Lrp4 protein and stimulates association between Lrp4 and the first immunoglobulin-like domain in muscle-specific kinase (MuSK). *J Biol Chem* **286:** 40624–40630.

Zhang B, Liang C, Bates R, Yin Y, Xiong WC, Mei L. 2012. Wnt proteins regulate acetylcholine receptor clustering in muscle cells. *Mol Brain* **5:** 7.

Diverging roles for Lrp4 and Wnt signaling in neuromuscular synapse development during evolution

Leonor Remédio, Katherine D. Gribble, Jennifer K. Lee, et al.

Genes Dev. 2016, **30:**
Access the most recent version at doi:10.1101/gad.279745.116